The Aromatic "Trapping" of the Catalytic Histidine Is Essential for Efficient Catalysis in Acetylcholinesterase†

Dov Barak,§ Dana Kaplan,‡ Arie Ordentlich,‡ Naomi Ariel,‡ Baruch Velan,‡ and Avigdor Shafferman*,‡

Departments of Organic Chemistry and Biochemistry & Molecular Genetics, Israel Institute for Biological Research, Ness-Ziona, 74100, Israel

Received February 19, 2002; Revised Manuscript Received April 29, 2002

ABSTRACT: While substitution of the aromatic residues (Phe295, Phe338), located in the vicinity of the catalytic His447 in human acetylcholinesterase (HuAChE) had little effect on catalytic activity, simultaneous replacement of both residues by aliphatic amino acids resulted in a 680-fold decrease in catalytic activity. Molecular simulations suggested that the activity decline is related to conformational destabilization of His447, similar to that observed for the hexamutant HuAChE which mimics the active center of butyrylcholinesterase. On the basis of model structures of other cholinesterases (ChEs), we predicted that catalytically nonproductive mobility of His447 could be restricted by introduction of aromatic residue in a different location adjacent to this histidine (Val407). Indeed, the F295A/F338A/V407F enzyme is 170-fold more reactive than the corresponding double mutant and only 3-fold less reactive than the wild-type HuAChE. However, analogous substitution of Val407 in the hexamutant HuAChE (generating the heptamutant Y72N/Y124Q/W286A/F295L/F297V/Y337A/V407F) did not enhance catalytic activity. Reactivity of these double, triple, hexa, and hepta mutant HuAChEs was monitored toward covalent ligands such as organophosphates and the transition state analogue TMFTA, which probe, respectively, the facility of the enzymes to accommodate Michaelis complexes and to undergo the acylation process. The findings suggest that in the F295A/F338A mutant the two His447 conformational states, which are essential for the different stages of the catalytic process, seem to be destabilized. On the other hand, in the F295A/F338A/V407F mutant only the state involved in acylation is impaired. Such differential effects on the His447 conformational properties demonstrate the general role of aromatic residues in cholinesterases, and probably in other serine hydrolases, in "trapping" of the catalytic histidine and thereby in optimization of catalytic activity.

The catalytic perfection of cholinesterases[1] (ChEs) is related to the optimized juxtaposition of the catalytic triad [Ser203(199); His447(440); Glu334(327)],[2] which is involved in the proton-transfer steps taking place during the acylation and deacylation processes (*1*, *2*). Mutagenesis studies in acetylcholinesterase (AChE) demonstrated that the exact positioning of the catalytic histidine (*3*−*5*), relative to other elements of the catalytic triad, is imperative for optimal hydrolytic activity (*4*). The precise positioning of the catalytic histidine is achieved through an array of interactions with acidic and aromatic residues adjacent to the active center (*6*−*8*). Enhanced conformational mobility of the catalytic histidine His447 was recently implicated in the activity differences between human butyrylcholinesterase (HuBChE) and the hexamutant human acetylcholinesterase (HuAChE) carrying aliphatic replacements of all the active site gorge aromatic residues (Tyr72; Tyr124; Trp286; Phe295; Phe297; Tyr337 HuAChE numbering) distinguishing between the two enzymes (*7*). The hexa-HuAChE mutant seems to mimic the active center architecture of HuBChE, displaying a HuBChE-like affinity toward *noncovalent* ligands (*7*). Yet, it exhibits a marked decrease in catalytic activity relative to either HuBChE or HuAChE. This activity difference was attributed to the impaired capacity of the hexamutant HuAChE to stabilize the tetrahedral intermediates emerging during the catalytic process, due to a suboptimal accommodation by the catalytic His447. Since no such impairment is evident in the case of HuBChE, it appears that different residues are involved in maintaining the optimal positioning of the catalytic histidine in AChE and in butyrylcholinesterase

† This work was supported by the U. S. Army Research and Development Command, Contract DAMD17-96-C-6088 and DAMD17-00-C-0021 (to A.S.).

* Corresponding author: Avigdor Shafferman, IIBR, Ness-Ziona, 74100, Israel. Tel (972)-8-9381595; Fax (972)-8-9401404; e-mail avigdor@iibr.gov.il.

§ Department of Organic Chemistry.

‡ Department of Biochemistry & Molecular Genetics.

[1] Abbreviations: ChE, cholinesterase; AChE, acetylcholinesterase; ACh, acetylcholine; HuAChE, human acetylcholinesterase; HuBChE, human butyrylcholinesterase; TcAChE *Torpedo californica* acetylcholinesterase; BChE, butyrylcholinesterase; DFP, diisopropyl phosphorofluoridate; tacrine, 9-amino-1,2,3,4-tetrahydroacridine hydrochloride hydrate; ATC, acetylthiocholine; edrophonium, ethyl(*m*-hydroxyphenyl)dimethylammonium chloride; BW284C51 1,5-bis(4-allyldimethylammoniumphenyl)pentan-3-one dibromide; 2-PAM, 2-hydroxyiminomethyl-1-methylpyridinium chloride; TMTFA, *m*-(*N*,*N*,*N*-trimethylammonio)trifluoro-acetophenone; HI-6, 1-(2-hydroxyiminomethylpyridinium)-1-(4-carboxyminopyridinium) dimethyl ether dichloride; soman, 1,2,2-trimethylpropyl methylphosphonofluoridate; Vx, *O*-ethyl-*S*-{2[bis[1-methylethyl)amino]ethyl}methyl-phosphonothioate.

[2] Amino acids and numbers refer to HuAChE, and the numbers in parentheses refer to the positions of analogous residues in TcAChE according to the recommended nomenclature (*41*).

10.1021/bi020143t CCC: $22.00
Published on Web 06/07/2002

(BChE). The importance of proper juxtaposition of His447 by aromatic residues in the HuAChE active center was also suggested by the large decrease in the rate of "aging" of phosphyl-F338A HuAChE conjugates compared to that of the wild-type enzyme (*8*). The aging process in phosphyl-ChE conjugates is usually attributed to the loss of alkyl group from the phosphyl alkoxy substituent, through scission of the alkyl-oxygen bond and formation of a carbonium ion (*8*−*10*). Its efficiency is believed to be critically dependent upon effective proton transfer to the alkoxy oxygen from the protonated histidine of the catalytic triad (*8*). In HuAChE, the optimal juxtaposition of this proton donor with the phosphyl moiety was found to include interaction with residue Phe338 (*8*, *11*). Interestingly, the efficiency of the aging process of the DFP adduct of HuBChE was not affected by aliphatic replacements of the aromatic residue Phe329 of HuBChE, which corresponds to Phe338 in HuAChE (*12*). This suggests again that in HuAChE and in HuBChE the conformational properties of the catalytic histidine are determined by a somewhat different set of interactions.

Actual movement of the catalytic histidine, in apparent response to steric changes in the active center, has recently been observed in the X-ray structure of the TcAChE-VX conjugate (*6*). It appears that the His440 side chain can move, through conformational adjustment, between the carboxylic acids Glu327 and Glu199, forming a tripartite array E327−H440−E199, which persists through most of the span of this motion. This array may be a structural device for orienting the imidazole according to the altered steric and electrostatic environment induced by the specific ligand bound to Ser200, and may account for the wide range of substrates hydrolyzed by ChEs.

In the present study, we further explored the nature of the putative array of interactions that optimize the orientation of the catalytic His447 with respect to other residues in the HuAChE active center. We found the minimal set of replacements that destabilize residue His447, resulting in decline of catalytic activity, and discovered how reactivity can be restored through careful design of its aromatic environment.

MATERIALS AND METHODS

Enzymes Reagents and Inhibitors. Mutagenesis of AChE was performed by DNA cassette replacement into a series of HuAChE sequence variants, which conserve the wild-type coding specificity (*13*), but carry new unique restriction sites (*14*−*16*). Generation of mutants F295A, Y337F, Y337A, F338A, and the hexamutant Y72N/Y124Q/W286A/F295L/F297V/Y337A was described previously (*7*, *17*, *18*). Construction of the double mutant F295A/F338A was carried out by replacements of the SalI−DdeI as well as the DdeI−Bsu36I DNA fragments of the AChE-w7 variant (*17*) with the respective fragments from the F295A and F338A variants. The double mutants Y337A/F338A and Y337F/F338A were generated by replacements of the MluI−NarI DNA fragment of the AChE-w7 cDNA variant (*17*) with the respective synthetic DNA duplexes carrying the mutated codons of Y337A/F338A and Y337F/F338A. The TAT codon of Tyr337 was changed to GCC(Ala) or TTC(Phe) and the TTC codon of Phe338 to GCC(Ala).

Generation of Y72N/Y124Q/W286A/F295L/F297V/Y337A/V407F was carried out by replacement of the Bsu36I−SpeI DNA fragment of the mutated neo-cat Y72N/Y124Q/W286A/F295L/F297V/Y337A vector (*7*) with the Bsu36I−BstBI synthetic DNA duplexes carrying V407F mutation and the BstBI−SpeI DNA fragment of the AChE-w3 variant (*16*). In the synthetic fragment, the GTC codon of Val407 was changed to TTC(Phe). Construction of the triple mutant F295A/F338A/V407F was carried out by replacing the HindIII−BglII DNA fragment of the neo-cat mutated vector, Y72N/Y124Q/W286A/F295L/F297V/Y337A/V407F (*7*), with the respective fragment of the F295A/F338A variant, carrying the two mutations.

All the synthetic DNA oligodeoxynucleotides were prepared using the automatic Applied Biosystems DNA synthesizer. The sequences of all clones were verified by the ABI PRISM BigDye terminator reaction kit, using the ABI310 genetic analyzer (Applied Biosystems).

Procedures of transfection of human embryonal kidney-derived cell line (HEK-293) with expression vectors of recombinant enzymes and the generation of stable cell clones, expressing high levels of each of the various recombinant products, were described previously (*14*−*16*).

Acetylthiocholine iodide (ATC), 5,5′-dithiobis (2-nitrobenzoic acid) (DTNB), ethyl(*m*-hydroxyphenyl)dimethylammonium chloride (edrophonium), 2-hydroxyiminomethyl-1-methylpyridinium chloride (2-PAM), 1,5-bis(4-allyldimethylammoniumphenyl)pentan-3-one dibromide (BW284C51), and diisopropyl phosphorofluoridate (DFP) were purchased from Sigma. *m*-(*N*,*N*,*N*-Trimethylammonio)trifluoro-acetophenone (TMTFA) was prepared according to the procedure described by Nair et al. (*19*), and 1-(2-hydroxyiminomethylpyridinium)-1-(4-carboxyminopyridinium) dimethyl ether dichloride (HI-6) was a gift from Dr. G. Amitai.

Preparation of the racemic mixtures of 1,2,2-trimethylpropyl methylphosphonofluoridate (soman) followed an accepted procedure using methylphosphonodifluoride and the appropriate alcohol (*20*).

Determination of HuAChE Activity and Analysis of Kinetic Data. Activity of HuAChE enzymes was assayed according to Ellman et al. (*21*) (in the presence of 0.1 mg/mL BSA, 0.3 mM DTNB, 50 mM sodium phosphate buffer pH-8.0 and various concentrations of ATC or BTC), carried out at 27 °C and monitored by a Thermomax microplate reader (Molecular Devices). Enzyme concentration was determined by ELISA (*16*) and by active-site titration (*15*) using purified P*s*C*s*-soman stereomer (*22*, *23*).

Michaelis−Menten constants (K_m) and the apparent first-order rate constants k_{cat} were determined according to the kinetic treatment described before (*16*, *17*). The apparent bimolecular rate constants k_{app} were calculated from the ratio k_{cat}/K_m.

Values of competitive inhibition constants (K_i) for the noncovalent inhibitors, edrophonium, tacrine, and BW284C51, were determined from the effects of various concentrations of the inhibitor on K_m and V_{max} of the enzyme-catalyzed hydrolysis of ATC. All the HuAChE enzymes examined formed rapid equilibria with the inhibitors, allowing for an immediate addition of increasing amounts of ATC to the enzyme−inhibitor mixture. The values of K_i were computed from the secondary plots of the apparent values of K_m vs concentrations of the respective inhibitors as described before (*18*).

The apparent first-order rate constants for the time-dependent inhibition of the wild-type HuAChE mutants by TMTFA were determined by periodical measurement of the initial rate of substrate hydrolysis of aliquots taken from the reaction mixture. Following the kinetic treatment described by Nair et al. (*19*, *24*) and assuming a two states inhibition mechanism, the values of k_{on} and k_{off} could be estimated from the linear plots of k_{obs} vs inhibitor concentration, according to eq 1.

$$k_{obs} = k'_{on}\,[\mathrm{TMTFA}] + k_{off} \quad (1)$$

Since in aqueous solution TMTFA is a mixture of the free ketone ($TMTFA_{ket}$) and the ketone hydrate ($TMTFA_{hyd}$), corrected values of the association rate constants were obtained from $k_{on} = k'_{on}(1 + [TMTFA_{hyd}]/[TMTFA_{ket}])$, using the ratio of hydrated and ketone forms of TMTFA (62500) as determined by ^{19}F NMR (*19*).

Measurements of phosphylation rates were carried out in at least four different concentrations of DFP or soman (I), and residual enzyme activity (*E*) at various time points was monitored. Pseudo-first-order phosphylation rate constants (k_i) were determined as the slopes of the plots of ln(*E*) versus time at different inhibitor concentrations. Bimolecular phosphylation rate constants were determined from plots of $\ln\{E/[I_o - (E_o - E)]\}$ versus time (*23*). Stereoselectivity of the enzymes toward various phosphonates, was determined by active-site titrations, comparing residual activities of enzymes inhibited by the appropriate racemic phosphonate to that of soman stereomer P*s*C*s* (*7*, *26*).

Measurements of aging rates, for HuAChE and its mutants, were determined after inhibition of 98% of the initial enzyme activity with soman. The inhibited enzymes were obtained under conditions where the rate of phosphonylation is much faster than the rate of aging. Excess soman was rapidly removed by column filtration (Sephadex G-15) or by 2-fold dilution prior to reactivation. The non-aged soman conjugate fraction was assessed by reactivation with 10 mM 2-PAM or HI-6 (under conditions where the rate of reactivation is faster than the rate of aging, *25*) that after 2 h was removed by column filtration (Sephadex G-15). The first-order rate constants of aging (k_a) were determined from slopes of $\ln(E_r)$ vs time.

Molecular Dynamics Simulation. Simulations of the wild-type, F295A/Y337A, F295A/F338A, and F295A/F338A/V407F HuAChEs were performed, as described before (*7*), on an Octane R12000 Silicon Graphics workstation using the Dynamics execution and analysis modules of SYBYL 6.6 (Tripos 1999). AMBER all-atom parameter set was used throughout the simulations. The starting conformation of the wild-type enzyme was obtained from the X-ray structure of the HuAChE-fasciculin complex model (*26*, structure 1b41 in the Protein Data Bank). The essential water molecules W659 and W670 (*26*) were retained throughout the simulations. Models of the HuAChE mutants were obtained by relaxation of the appropriately modified structures. Between 148 and 155 residues were involved in the simulation, while the rest of the structure was constrained (the small changes in the number of residues involved in the simulation had no effect on the conformational behavior in the active center). Initial equilibrations at 300 K (20 ps) were followed by 160 ps of dynamics runs at 400 K with constrained main chain.

Table 1: Rate Constants[a] of Substrate Hydrolysis and "Aging" of Somanyl Adducts of HuAChE and Its Mutants

	ATC			aging soman
AChE type	K_m (mM)	k_{cat} ($\times 10^{-5}$ min^{-1})	k_{cat}/K_m ($\times 10^{-8}$ M^{-1} min^{-1})	k_a (pH 8; 24 °C) ($\times 10^3$ min^{-1})
WT	0.15	5.1	34.0	37
F295A	0.13	3.8	29.0	8.8
Y337A	0.10	1.4	14.0	15
Y337F	0.18	4.0	22.6	54
F338A	0.24	2.4	10.0	0.3
Y337A/F338A	0.12	2.4	20.0	ND[b]
Y337F/F338A	0.15	2.3	15.0	ND[b]
F295A/F338A	4.9	0.24	0.05	0.3
F295A/F338A/V407F	0.07	0.6	9.0	5

[a] Values represent means of triplicate determinations with standard deviation not exceeding 20%. [b] Not determined.

Simulations of the hexamutant (Y72N/Y124Q/W286A/F295L/F297V/Y337A) and the heptamutant (Y72N/Y124Q/W286A/F295L/F297V/Y337A/V407F) HuAChEs were performed using the AMBER 5.0 suite of programs with all atom parameter set (*27*). Initial equilibration 300 K (20 ps) was followed by 200 ps of dynamics run at 400 K with AMBER belly option comprising of 96 residues within the active center gorge and its vicinity (*28*).

RESULTS AND DISCUSSION

The finding that the hexamutant HuAChE does not mimic the reactivity of HuBChE toward substrates and other covalent ligands suggested that the catalytically productive orientation of His447 cannot be fully maintained in the mutated enzyme (*7*). Yet, the specific interactions with His447, which were apparently abolished during the massive reorganization of the active center, could not be identified. To further investigate the relationship between the conformational mobility of the catalytic His447 and the reactivity characteristics of HuAChE enzymes, we looked for more localized structural perturbations in the immediate vicinity of position 447. According to the X-ray structure of HuAChE (*26*), the catalytic His447 is within interaction distance to the aromatic residues Phe295, Phe338, and Tyr337. Yet, single replacements of these aromatic residues, by alanine, had only a marginal effect on the catalytic activity of the resulting mutant enzymes (*11*, *18*). Thus, in a further attempt to perturb the aromatic environment of His447, the double HuAChE mutants F295A/F338A and Y337A/F338A were generated. With respect to catalytic activity, the Y337A/F338A enzyme displayed a similar phenotype to that of the wild-type and the F338A HuAChEs (Table 1). On the other hand, for the F295A/F338A enzyme, a very dramatic decrease of catalytic activity toward ATC was observed, with a 680-fold diminished bimolecular rate constant (5×10^6 M^{-1} min^{-1}) compared to that of the wild-type enzyme. This decline in catalytic activity of the double mutant does not result from major changes in the overall architecture of the active center since affinities of the F295A/F338A enzyme toward the active center inhibitors tacrine, BW284C51, and edrophonium were either equivalent to, or merely 5-fold lower than, those of the wild-type HuAChE (Table 2).

The possible relation between the diminished hydrolytic activity of the F295A/F338A HuAChE and the enhanced

Table 2: Inhibition Constants[a] of Selected Ligands with HuAChE and Its Mutants

AChE type	edrophonium K_i μM	tacrine K_i nM	BW284C51 K_i nM	TMTFA k_{on} ($\times 10^{-9}$ M^{-1} min^{-1})	DFP k_i ($\times 10^{-4}$ M^{-1} min^{-1})	soman k_i ($\times 10^{-4}$ M^{-1} min^{-1})
WT	0.3	60	10	190	10	10000
F295A	0.2	45	3.5	130	45	3600
Y337A	2.5	6	50	130	2	3400
Y337F	0.3	150	11	160	30	5600
F338A	0.3	30	10	400	2	10000
Y337A/F338A	1.5	ND	ND	80	6	9300
Y337F/F338A	0.8	40	17	100	3	20000
F295A/F338A	1.5	50	10	20	4	100
F295A/F338A/V407F	1.5	100	25	20	50	1500

[a] Values represent means of triplicate determinations with standard deviation not exceeding 20%.

Table 3: Kinetics Constants of the Hexa- and Heptamutant HuAChEs

AChE type	ATC k_{app} ($\times 10^{-8}$ M^{-1} min^{-1})	edrophonium K_i (μM)	tacrine K_i (nM)	BW284C51 K_i (nM)	TMTFA k_{on} ($\times 10^{-9}$ M^{-1} min^{-1})	DFP k_i ($\times 10^{-4}$ M^{-1} min^{-1})	soman k_i ($\times 10^{-4}$ M^{-1} min^{-1})	aging soman k_a (pH 8; 24 °C) ($\times 10^3$ min^{-1})
WT	34.0 (1)	0.3 (1)	60 (1)	10 (1)	190 (1)	10 (1)	10000 (1)	37 (1)
[Y72N/Y124Q/ W286A/F295L/ F297V/Y337A]	0.2 (170)[a]	50 (0.01)	12 (5)	170000 (0.0001)	1 (190)	1500 (0.01)	50 (200)	<0.3 (>100)
[Y72N/Y124Q/ W286A/F295L/ F297V/Y337A/ V407F]	0.2 (170)	35 (0.01)	20 (3)	ND[b]	0.7 (270)	270 (0.05)	380 (25)	ND[b]

[a] The number in parentheses represents the ratio between the rate constant of WT HuAChE to that of the rate constants of the corresponding mutant. [b] Not determined.

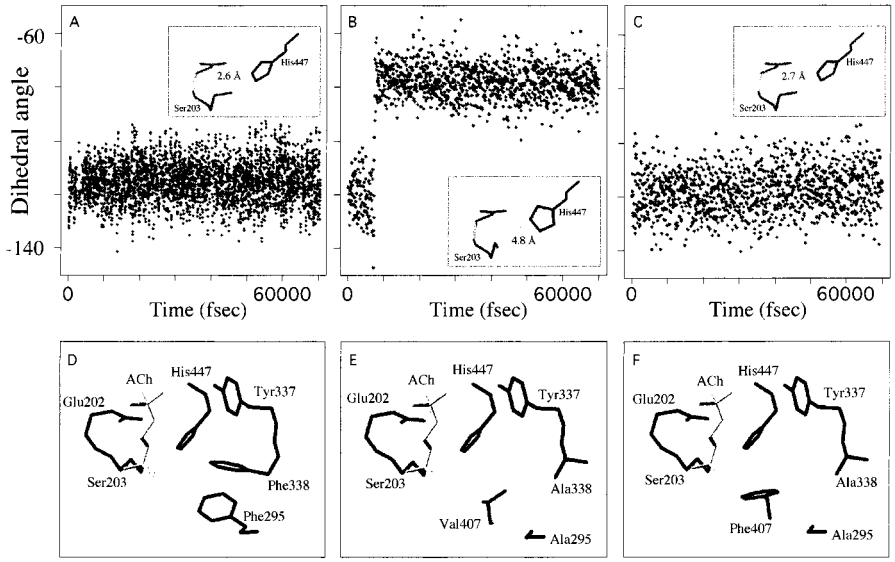

FIGURE 1: Conformational mobility and aromatic "caging" of the catalytic histidine side chain. Molecular dynamics simulations performed on (A) wild-type HuAChE, (B) F295A/F338A HuAChE, and (C) F295A/F338A/V407F HuAChE. Respective time dependencies of the dihedral angles between the imidazolium moiety and the backbone are depicted. For each simulation, the corresponding equilibrium juxtapositions, of the catalytic His447 and Ser203, are shown in the insets. Putative "caging" of His447 by aromatic residues is shown for HuAChE-ACh tetrahedral intermediates of (D) the wild-type enzyme, (E) the F295A/F338A mutant, and (F) the F295A/F338A/V407F mutant.

mobility of the His447 side chain was examined by molecular simulation of residue motions at the active center. The starting structure used in these experiments was taken from the X-ray structure of the HuAChE−fasciculin complex (*26*), by removing the ligand and relaxing the regions of contact (*7*). The results seem to suggest that indeed in the catalytically impaired F295A/F338A HuAChE, the His447 side chain tends to assume a different average conformation (see Figure 1B) from that observed in the X-ray structure of HuAChE (Figure 1A). This conformational transition may affect the capability of His447 to accommodate tetrahedral intermediates and therefore diminish the reactivity of the enzyme toward covalent modifiers (see inset Figure 1B). On the other hand, in the F338A or F295A as well as in the F337A/F338A enzymes, the side chain of His447 maintained the same average orientation as that in the wild-type HuAChE (in all these enzymes the average dihedral angle between the imidazolium moiety of His447 and the backbone was 115−(−125°) throughout the simulations).

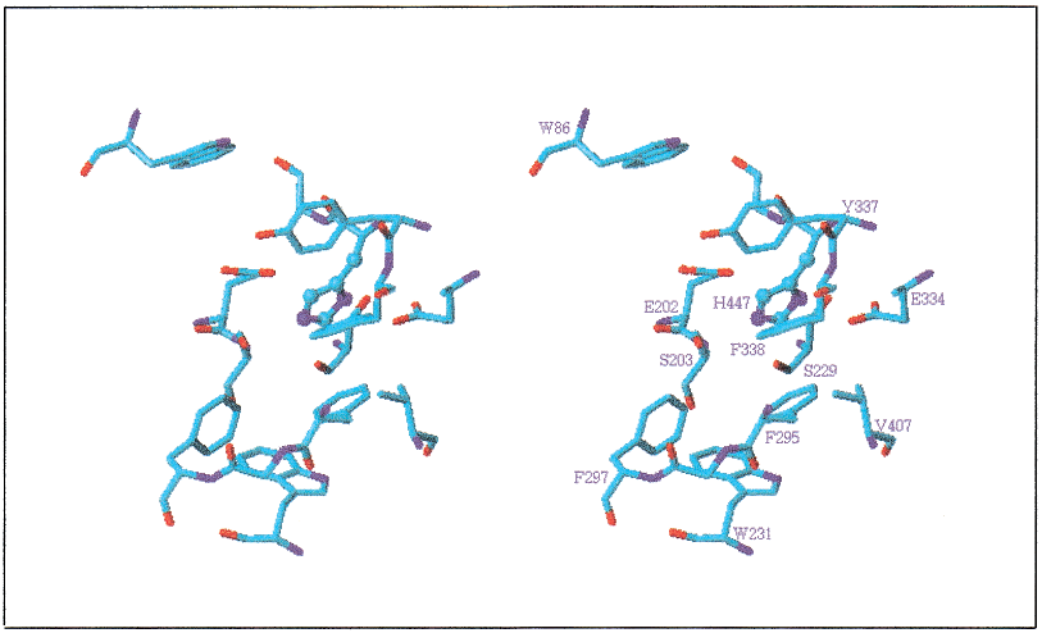

FIGURE 2: Stereoview of residues surrounding the catalytic His447 in the HuAChE active center. Heteroatoms are color coded and the side chain of His447 is shown in ball and stick representation.

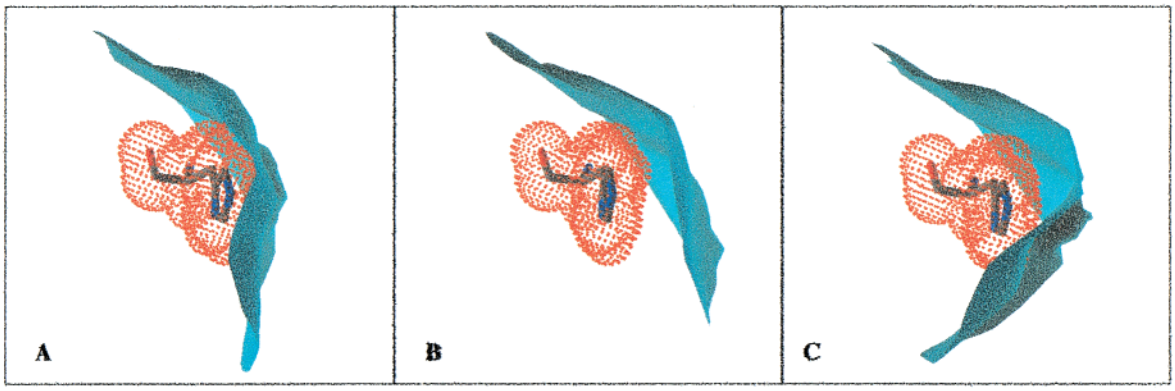

FIGURE 3: Complementarity of the van der Waals surfaces of His447 (depicted as dot surface) and adjacent residues at positions 337, 338, 295, and 407 (shown as solid surface) is illustrated for (A) the wild-type; (B) F295A/F338A; and (C) F295A/F338A/V407F HuAChEs. Note that removal of aromatic residues from the vicinity of the His447 side chain leaves a void (illustrated in panel B) that allows for its enhanced conformational mobility. Introduction of aromatic residue in position 407 partially restores the complementarity between the van der Waals surfaces (illustrated in panel C).

If the enhanced mobility of His447 in F295A/F338A HuAChE and the ensuing decrease of catalytic activity are related directly to elimination of stabilizing interactions with the two *aromatic* residues, it seemed reasonable to assume that a compensatory interaction could be engineered through introduction of an aromatic residue in a different location adjacent to His447. This notion gains support from the wild-type-like phenotype of the F329A HuBChE with respect to aging of the BChE−DFP conjugate (*12*). The F329A HuBChE is actually analogous to the F295L/F338A HuAChE, since in HuBChE residues Leu286 and Phe329 correspond to Phe295 and Phe338 in HuAChE. Examination of the HuAChE/HuBChE sequence similarity and of molecular models of the two cholinesterases showed that in HuBChE an aromatic residue Phe398 appears to be vicinal to the catalytic histidine. In HuAChE, the residue in equivalent position to Phe398 is Val407, which due to its size does not seem to interact with His447 (Figure 2). We hypothesized therefore that introduction of phenylalanine at position 407 of the F295A/F338A HuAChE could compensate for the enhanced mobility of His447 in the double mutant and thereby for the loss in catalytic activity (Figure 3). This notion was initially tested by molecular dynamics simulation of side chain mobility within the active center of the F295A/F338A/V407F enzyme. As shown in Figure 1C, the conformational properties of His447 in the "theoretical" triple mutant indeed resemble those of the wild-type enzyme rather than those of the F295A/F338A HuAChE (Figure 1A,B). This prediction was fully realized when the F295A/F338A/V407F HuAChE was actually generated and produced, since its catalytic activity was indeed 180-fold higher than that of the F295A/F338A enzyme and only 3.5-fold lower than that of the wild-type HuAChE (see Table 1). Moreover, catalysis of the aging process of the HuAChE F295A/F338A/V407−soman adduct was also more efficient than that of the corresponding adduct of the F295A/F338A HuAChE (Table 1). It appears therefore that phenylalanine at position 407 may indeed restrict the conformational mobility of His447 and can thus partially compensate for the loss of aromatic residues at positions 295 and 338 (Figure 3). Interestingly,

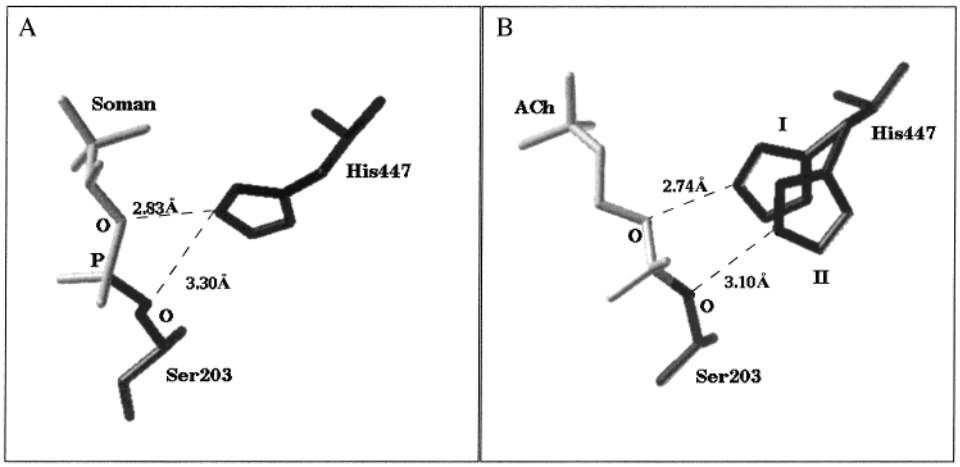

FIGURE 4: Putative functional states of residue His447. (A) The conformation of His447 participating in the aging process of HuAChE−soman conjugate (*8*). (B) Conformational states of His447 that may participate in the catalysis of substrate hydrolysis, as manifested by distances from the oxygen atoms of the tetrahedral intermediate. Conformation I proximal to the alkoxy oxygen (and 3.4 Å away from O^{γ}-Ser203) may be involved in the release of choline from the ACh-AChE tetrahedral intermediate. Conformation II proximal to O^{γ}-Ser203 (and 3.6 Å away from the alkoxy oxygen) is probably involved in enzyme release from the hydrated acyl-enzyme.

while this conformational restriction results in complete restoration of the value of Michaelis Menten constant K_m (actually it is 2-fold lower than that of the wild-type enzyme), the corresponding value of k_{cat} is only 2-fold higher than that of the F295A/F338A enzyme and still 9-fold lower compared to that of the WT HuAChE (Table 1). Therefore, in the triple mutant the capacity of His447 to accommodate the noncovalent complex of ATC is similar to that of the wild-type HuAChE. On the other hand, the triple mutant enzyme seems nearly as impaired as the F295A/F338A HuAChE with respect to the covalent bond formation step, suggesting that different properties of His447 may be involved in the two processes.

To further test this hypothesis, we compared the reactivities of the F295A/F338A and the F295A/F338A/V407F HuAChEs toward the active center irreversible phosphate inhibitors soman and DFP and the transition state analogue TMTFA. It is well established that in AChEs initial formation of noncovalent Michaelis complexes with phosphate inhibitors precedes the much slower covalent reaction with the enzyme (*29*−*32*). Thus, the observation that the inhibition rate constants (k_i) of the F295A/F338A/V407F HuAChE by soman and DFP are 15- and 13-fold higher than the respective values for the F295A/F338A enzyme (Table 2) is consistent with the effect of the corresponding mutations on the values of K_m. On the other hand, in reactions with TMTFA, which involve rapid formation of covalent tetrahedral intermediate (*19*, *24*, *33*), the F295A/F338A and the F295A/F338A/V407F HuAChEs yielded similar kinetic constants. Thus, it seems that with respect to the acylation process, the loss of His447 "caging" by aromatic residues Phe295 and Phe338 in wild-type HuAChE is not compensated for by introduction of an aromatic residue at position 407 (Figure 1D−F).

The finding that introduction of aromatic residue at position 407 of HuAChE partially compensates for the perturbation introduced in the immediate aromatic environment of His447 by replacement of residues Phe295 and Phe338 raised the possibility that similar effect could be achieved for the "butyryl-like" hexamutant HuAChE. Although in the latter, the enhanced mobility of His447 cannot be attributed to specific residue replacements, but rather it seems to be a nonspecific consequence of void creation in the active center (*7*). Indeed, the hexamutant HuAChE seems to be slightly more impaired than the F295A/F338A enzyme in accommodating the Michaelis complex of soman and is considerably less reactive toward TMTFA. Furthermore, the hexamutant displayed also ~30-fold lower affinity than the F295A/F338A HuAChE toward the noncovalent inhibitor edrophonium.

Preliminary examination of the effect of aromatic replacement at position 407, on the conformational properties of His447, was carried out by molecular simulation on the theoretical model of the Y72N/Y124Q/W286A/F295L/F297V/Y337A/V407F (heptamutant) HuAChE. The results suggest that the mobility of the His447 side chain is qualitatively similar to that in the hexamutant HuAChE. Thus, unlike the case of the F295A/F338A/V407F enzyme, introduction of aromatic residue adjacent to His447 failed to restrict its mobility to the extent that could be observed in our simulations. Such prediction was found consistent with the experimentally observed catalytic activity of the heptamutant HuAChE, which was nearly equivalent to that the hexamutant enzyme (Table 3). The hepta- and the hexamutants showed also equivalent reactivity toward TMTFA and nearly equivalent affinity toward edrophonium and tacrine. Thus, with respect to the overall architecture of the active center and the conformational properties of His447 during the acylation process, the heptamutant resembles closely the hexamutant HuAChE (Table 3). On the other hand, the heptamutant was 8-fold more reactive toward soman compared to the hexamutant HuAChE, suggesting again that in cases where reactivity is determined predominantly by accommodation of the corresponding Michaelis complex, the participation of His447 can be augmented to some extent by aromatic substitution at position 407.

The case of DFP is particularly interesting since it demonstrates the interplay of different effects on the stabilization of the respective Michaelis complexes. In the recently reported X-ray structure of the aged DFP−TcAChE conjugate, both the acyl pocket and parts of the peripheral anionic site seem distorted due to the interactions with the

phosphoryl isopropoxy substituent (*34*). Some of such severe steric congestion in the DFP-wild-type HuAChE Michaelis complex is relieved in the corresponding complex with the F295A enzyme (*31*). In the complex with the F295A/F338A HuAChE, this stabilizing effect is offset by the suboptimal interaction with residue His447. When this interaction is fully restored (in the corresponding complex with the F295A/F338A/V407F enzyme), the stability of the resulting complex is practically equivalent to that of the F295A enzyme. On the other hand, while replacement of aromatic residues at the active center and at the peripheral anionic site of the hexamutant HuAChE was beneficial for the steric accommodation of DFP (*7*), the respective DFP Michaelis complex of the heptamutant seems to be less stable.

Motion of the imidazole moiety of catalytic histidine between the two positions, proximal to the heteroatom of the leaving group and to the O^{γ}-atom of the catalytic serine (e.g., states I and II, respectively, see Figure 4B), was suggested in the past as an integral part of the catalytic machinery in HuAChE (*6*, *8*), as well as in other serine hydrolases (*35*), operating both in acylation and deacylation steps. However, since the driving force for such movement is not yet understood (*36*), its necessity for the enzymatic activity is not generally accepted (*37*). The results of the present study appear to suggest that in HuAChE residue His447 assumes two distinct functional states, with somewhat different orientations relative to the immediate molecular environment. One of these states, involved in accommodation of noncovalent Michaelis complexes and in the "aging" mechanism of phosphylated HuAChEs (see Figure 4A), may correspond to conformation I in Figure 4B. The other functional state participates in bond formation processes and may resemble conformation II in Figure 4B. In each of these functional states, the imidazole moiety of His447 is uniquely "caged" by adjacent aromatic residues in the active center, which include Phe295, Phe338 as well as Phe297 and Tyr337 (see Figure 1D and ref *7*). Local perturbation of the His447 aromatic environment, as in the F295A/F338A enzyme, or a more extensive reorganization of the active center, as in the hexa- and the heptamutant HuAChEs, result in mobility enhancement of His447 in both functional states. In contrast, the F295A/F338A/V407F enzyme presents a unique case where differential "caging" of the two states could be resolved. Such differential effects on the His447 conformational properties demonstrate that apart from the electrostatic influence of the two adjacent glutamates [Glu*199*(202) and Glu*327*(334)] (*1*, *6*, *11*, *38*), caging by aromatic residues may play a general role in the exact positioning of the catalytic histidine (through $\pi-\pi$ and cation$-\pi$ interactions) and thereby in optimization of catalytic activity of cholinesterases, and possibly also in other hydrolases (*39*, *40*).

REFERENCES

1. Fuxreiter, M., and Warshel, A. (1998) *J. Am. Chem. Soc. 120*, 183−194.
2. Vagedes, P., Rabenstein, B., Aquist, J., Marelius, J., and Knapp, E.-W. (2000) *J. Am. Chem. Soc. 122*, 12254−12262.
3. Gibney, G., Camp, S., Dionne, M., MacPhee-Quigley, K., and Taylor, P. (1990) *Proc. Natl. Acad. Sci. U.S.A. 87*, 7546−7550.
4. Shafferman, A., Kronman, C., Flashner, Y., Leitner, M., Grosfeld, H., Ordentlich, A., Gozes, Y., Cohen, S., Ariel, N., Barak, D., Harel, M., Silman, I., Sussman J. L., and Velan, B. (1992) *J. Biol. Chem. 267*, 17640−17648.
5. Shafferman, A., Velan, B., Ordentlich, A., Kronman, C., Grosfeld, H., Leitner, M., Flashner, Y., Cohen, S., Barak, D., and Ariel, N. (1992) *EMBO J. 11*, 3561−3568.
6. Millard, C. B., Koellner, G., Ordentlich, A., Shafferman, A., Silman, I., and Sussman, J. L. (1999) *J. Am. Chem. Soc. 121*, 9883−9884.
7. Kaplan, D., Ordentlich, A., Barak, D., Ariel, N., Kronman, C., Velan, B., and Shafferman, A. (2001) *Biochmistry 40*, 7433−7445.
8. Shafferman, A., Ordentlich, A., Barak, D., Stein, D., Ariel, N., and Velan, B. (1996) *Biochem. J. 318*, 833−840.
9. Benschop, H. P., and Keijer, J. H. (1966) *Biochim. Biophys. Acta 128*, 586−588.
10. Michel, H. O., Hackley, B. E., Jr., Berkowitz, L., List, G., Hackley, E. B., Gilliam, W., and Paukan, M. (1967) *Arch. Biochem. Biophys. 121*, 29−34.
11. Ordentlich, A., Kronman, C., Barak, D., Stein, D., Ariel, N., Marcus, D., Velan, B., and Shafferman, A. (1993) *FEBS Lett. 334*, 215−220.
12. Masson, P., Fortier, P. L., Albaret, C., Froment, M. T., Bartels, C. F., and Lockridge, O. (1997) *Biochem. J. 327*, 601−607.
13. Soreq, H., Ben-Aziz, R., Prody, C. A., Seidman, S., Gnatt, A., Neville, L., Lieman-Hurwitz, J., Lev-Lehman, E., Ginzberg, D., Lipidot-Lifson, Y., and Zakut, H. (1990) *Proc. Natl. Acad. Sci. U.S.A. 87*, 9688−9692.
14. Velan, B., Grosfeld, H., Kronman, C., Leitner, M., Gozes, Y., Lazar, A., Flashner, Y., Marcus, D., Cohen, S., and Shafferman, A. (1991) *J. Biol. Chem. 266*, 23977−23984.
15. Kronman, C., Velan, B., Gozes, Y., Leitner, M., Flashner, Y., Lazar, A., Marcus, D., Sery, T., Papier, Y., Grosfeld, H., Cohen, S., and Shafferman, A. (1992) *Gene 121*, 295−304.
16. Shafferman, A., Kronman, C., Flashner, Y., Leitner, S., Grosfeld, H., Ordentlich, A., Gozes, Y., Cohen, S., Ariel, N., Barak, D., Harel, M., Silman, I., Sussman, J. L., and Velan, B. (1992) *J. Biol. Chem. 267*, 17640−17648.
17. Shafferman, A., Velan, B., Ordentlich, A., Kronman, C., Grosfeld, H., Leitner, M., Flashner, Y., Cohen, S., Barak, D., and Ariel, N. (1992) *EMBO J. 11*, 3561−3568.
18. Ordentlich, A., Barak, D., Kronman, C., Flashner, Y., Leitner, M., Segall, Y., Ariel, N., Cohen, S., Velan, B., and Shafferman, A. (1993) *J. Biol. Chem. 268*, 17083−17095.
19. Nair, H. K., Lee, K., and Quinn, D. M. (1993) *J. Am. Chem. Soc. 115*, 9939−9941.
20. Barak, D., Ordentlich, A., Segall, Y., Velan, B., Benschop, H. P., De Jong, L. P. A. and Shafferman, A. (1997) *J. Am. Chem. Soc. 119*, 3157−3158.
21. Ellman, G. L., Courtney, K. D., Andres, V., and Featherstone, R. M. (1961) *Biochem. Pharmacol. 7*, 88−95.
22. Benschop, H. P., Konings, C. A. G., Van Genderen, J., and De Jong, L. P. A (1984) *Toxicol. Appl. Pharmacol. 72*, 61−74.
23. Ordentlich, A., Barak, D., Kronman, C., Benschop, H. P., De Jong, L. P. A., Ariel, N., Barak, R., Segall, Y., Velan, B., and Shafferman, A. (1999) *Biochemistry 38*, 3055−3066.
24. Nair, H. K., Seravalli, J., Arbuckle, T., and Quinn, D. M. (1994) *Biochemistry 33*, 8566−8576.
25. Grosfeld, H., Barak, D., Ordentlich, A., Velan, B., and Shafferman, A. (1996) *Mol. Pharmacol. 50*, 639−649.
26. Kryger, G., Harel, M., Giles, K., Toker, L., Velan, B., Lazar, A., Kronman, C., Barak, D., Ariel, N., Shafferman, A., Silman, I., and Sussman, J. L. (2000) *Acta Crystallogr. D56*, 1385−1394.
27. Case, D. A., Pearlman, D. A., Caldwell, J. W., Chetham, T. E., Ross, W. S., Simmerling, C. L., Darden, T. A., Merz, K. M., Stanton, R. V., Cheng, A. L., Vincent, I. J., Crowley, M., Ferguson, D. M., Radmer, R. J., Seibel, G. L., Singh, U. C., Weiner, P. K., and Kollman, P. A. (1997) AMBER 5, University of California, San Francisco.
28. Velan, B., Barak, D., Ariel, N., Leitner, M., Bino, T., Ordentlich, A., and Shafferman, A. (1996) *FEBS Lett. 395*, 22−28.
29. Aldridge, W. N., and Reiner, E. *Enzyme Inhibitors as Substrate*s 1972, North Holland Publishing Co., Amsterdam.
30. Main, A. R. (1976) in *Biology of Cholinergic Function* (Goldberg, A. M., and Hanin, I., Eds.) pp 269−353, Raven Press New York.
31. Ordentlich, A., Barak, D., Kronman, C., Ariel, N., Segall, Y., Velan, B., and Shafferman, A. (1996) *J. Biol. Chem. 271*, 11953−11962.

32. Ordentlich, A., Barak, D., Marcus, D., Lazar, A., Benschop, H. P., De Jong, L. P. A., Ariel, N., Barak, R., Segall, Y., Velan, B., and Shafferman, A. (1999) *Biochemistry 38*, 3055−3066.
33. Ordentlich, A., Barak, D., Kronman, C., Ariel, N., Segall, Y., Velan, B., and Shafferman, A. (1998) *J. Biol. Chem. 273*, 19509−19517.
34. Millard, C. B., Kryger, G., Ordentlich, A., Greenblatt, H., Harel, M., Raves, M., Segall, Y., Barak, D., Shafferman, A., Silman, I., and Sussman, J. L. (1999) *Biochemistry 38*, 7032−7039.
35. Bachovchin, W. W. (1986) *Biochemistry 25*, 7751−7759.
36. Perona, J. J., Craik, C. S., and Fletterick, R. J. (1993) *Science 261*, 620−621.
37. Ash, E. L., Sudmeier, J. L., Day, R. M., Vincent, M., Torchlin, E. V., Haddad, K. C., Bradshaw, E. M., Sanford, D. G., and Bachovchin, W. W. (2000) *Proc. Natl. Acad. Sci. U.S.A. 97*, 10371−10376.
38. Massiah, M. A., Viragh, C., Reddy, P. M., Kovach, I., Johnson, J., Rosenberry, T. L., and Mildvan, A. S. (2001) *Biochemistry, 40*, 5682−5690.
39. Bromme, D., Bonneau, P. R., Purisima, E., Lachance, P., Hajnik, S., Thomas, D. Y., and Storer, A. C. (1996) *Biochemistry, 35*, 3970−3979.
40. Ghosh, D., Sawicki, M., Lala, P., Erman, M., Pangborn, W., Eyzaguirre, J., Gutierrez, R., Jornvall, H., and Thiel, D. J. (2001) *J. Biol. Chem. 276* 11159−11166.
41. Massoulie, J., Sussman, J. L., Doctor, B. P., Soreq, H., Velan, B., Cygler, M., Rotundo, R., Shafferman, A., Silman, I., and Taylor, P. (1992) in *Multidisciplinary Approaches to Cholinesterase Functions* (Shafferman, A., and Velan, B. Eds.) pp 285−288, Plenum Press, NY.

BI020143T